# Measurement of Analyzing Power for Proton-Carbon Elastic Scattering in the Coulomb-Nuclear Interference Region with a 22-GeV/$c$ Polarized Proton Beam

J. Tojo,[1,*] I. Alekseev,[2] M. Bai,[3] B. Bassalleck,[4] G. Bunce,[3,5] A. Deshpande,[5] J. Doskow,[6] S. Eilerts,[4] D. E. Fields,[4,5]
Y. Goto,[5,7] H. Huang,[3] V. Hughes,[8] K. Imai,[1] M. Ishihara,[5,7] V. Kanavets,[2] K. Kurita ,[5,†] K. Kwiatkowski,[6] B. Lewis,[4]
W. Lozowski,[6] Y. Makdisi,[3] H.-O. Meyer,[6] B. V. Morozov,[2] M. Nakamura,[1] B. Przewoski,[6] T. Rinckel,[6] T. Roser,[3]
A. Rusek,[3] N. Saito,[5,7,‡] B. Smith,[4] D. Svirida,[2] M. Syphers,[3,§] A. Taketani,[5,7] T. L. Thomas,[4] D. Underwood,[9] D. Wolfe,[4]
K. Yamamoto,[1,||] and L. Zhu[1,¶]

[1]Department of Physics, Kyoto University, Kyoto 606-8502, Japan
[2]Institute of Theoretical and Experimental Physics, 117259 Moscow, Russia
[3]Brookhaven National Laboratory, Upton, New York 11973
[4]Department of Physics and Astronomy, University of New Mexico, Albuquerque, New Mexico 87131
[5]RIKEN BNL Research Center, Upton, New York 11973
[6]Indiana University Cyclotron Facility, Bloomington, Indiana 47405
[7]RIKEN (The Institute of Physical and Chemical Research), Wako, Saitama 351-0198, Japan
[8]Department of Physics, Yale University, New Haven, Connecticut 06511
[9]Argonne National Laboratory, Argonne, Illinois 60439

The analyzing power for proton-carbon elastic scattering in the Coulomb-nuclear interference region of momentum transfer, $9.0 \times 10^{-3} < -t < 4.1 \times 10^{-2}$ $(\text{GeV}/c)^2$, was measured with a 21.7 GeV/$c$ polarized proton beam at the Alternating Gradient Synchrotron of Brookhaven National Laboratory. The ratio of hadronic spin-flip to nonflip amplitude, $r_5$, was obtained from the analyzing power to be $\text{Re} r_5 = 0.088 \pm 0.058$ and $\text{Im} r_5 = -0.161 \pm 0.226$.

The analyzing power, $\mathcal{A}_N$, defined by the left-right asymmetry of the cross sections in the scattering plane normal to the beam polarization, can arise only from the interference between a spin-flip and a nonflip amplitude and thus provides important information on the spin dependence of the interactions. In high energy proton-proton ($pp$) [1,2] and proton-nucleus ($pA$) [3,4] elastic scattering at very small momentum transfer, $\mathcal{A}_N$ originates from the interference between the electromagnetic (Coulomb) spin-flip and the hadronic (nuclear) nonflip amplitude. This analyzing power has been calculated to have a maximum value of about 4% around momentum transfer $-t = 2 \times 10^{-3}$ $(\text{GeV}/c)^2$ and to decrease as $|t|$ increases. $\mathcal{A}_N$ in this Coulomb-nuclear interference (CNI) region of momentum transfer has been suggested as a sensitive probe of the hadronic spin-flip amplitude [5]. The hadronic spin-flip amplitude is characterized by the ratio of the spin-flip to the nonflip amplitude, $r_5 = (m/\sqrt{-t}) \times F_s^h/\text{Im} F_o^h$, where $F_{o,s}^h$ are the hadronic parts of the spin-flip amplitude, $F_s$, and nonflip amplitude, $F_o$, and $m$ is the nucleon mass. The existence of the hadronic spin-flip amplitude introduces a deviation from $\mathcal{A}_N$ calculated with no hadronic spin-flip amplitude. There are theoretical estimates and experimental evidence for the possibility of a nonzero hadronic spin-flip amplitude reflecting helicity nonconservation in the direct channel of the reaction [2]. A hadronic spin-flip amplitude nonvanishing at high energies carries important physics information on static properties and on the constituent quark structure of the nucleon. In the framework of

Regge phenomenology, hadronic amplitudes surviving in the high energy asymptotic region are described by Pomeron exchange. The Regge pole model does not limit the value of the Pomeron spin-flip amplitude but leads to a vanishing contribution to $\mathcal{A}_N$ due to equal phases of the spin-flip and nonflip parts of the Pomeron exchange. $\mathcal{A}_N$ in the CNI region remains sensitive to the Pomeron spin-flip amplitude because of the phase difference between the hadronic and Coulomb amplitudes, which is close to $\pi/2$. As was pointed out by Kopeliovich and Trueman [4], the usage of a carbon target (an isoscalar nuclear target) has an important advantage of eliminating the contribution of the isovector Reggeons and thus allows one to probe the Pomeron spin-flip amplitude through $\mathcal{A}_N$ at medium high energies.

Measurement of $\mathcal{A}_N$ for proton-carbon ($p$C) elastic scattering in the CNI region has been proposed not only to investigate a hadronic spin-flip amplitude, but also to provide a method for high energy proton polarimetry at the Relativistic Heavy Ion Collider (RHIC) of Brookhaven National Laboratory (BNL) [6]. Predicted properties of $\mathcal{A}_N$ (large cross section and the weak $\sqrt{s}$-dependence) make this process ideal for beam polarization measurements at RHIC.

The E950 experiment at the Alternating Gradient Synchrotron (AGS) of BNL was carried out to measure $\mathcal{A}_N$ for $p$C elastic scattering in the CNI region at 21.7 GeV/$c$. The measurement was made in the AGS ring using an internal carbon target. We identified $p$C

elastic scattering by detecting only recoil carbon ions, which had energies ranging from 300 to 2000 keV and recoil angles of 89°–90° with respect to the beam direction. The forward scattered proton, at very small scattering angles, was not detected. In this Letter, we present the result of the measurement of $\mathcal{A}_N$ and the constraint on $r_5$.

The transversely polarized proton beam was accelerated in the AGS with the beam polarization preserved by a partial Siberian snake [7] and an rf dipole [8]. A flat-top of 520 ms in the AGS accelerating cycle was used for the experiment. The polarization direction was flipped for each AGS cycle to reduce systematic uncertainties in the $\mathcal{A}_N$ measurement. The beam was bunched so that we were able to determine the timing of a beam crossing at the carbon target and separate slow recoil carbon ions from prompt backgrounds. The AGS beam consisted of one bunch of about $6 \times 10^9$ protons with a width of $\sim 25$ ns and with a rotation period of 2.7 $\mu$s.

The beam polarization was measured concurrently by experiment BNL-AGS E925, based on the analyzing power of $pp$ elastic scattering at 21.7 GeV/$c$ and at $-t = 0.15 \pm 0.05$ (GeV/$c$)$^2$, $\mathcal{A}_N^{pp} = 0.0400 \pm 0.0048$ [9]. For each AGS cycle, the beam was debunched and was extracted to the CH$_2$ target of the polarimeter after the data taking time window for the E950 experiment. $pp$ elastic scattering was identified by detecting both scattered and recoil protons. The average beam polarization during the E950 experiment was determined to be $\mathcal{P}_B = 0.407 \pm 0.036$(stat) $\pm 0.049$(syst).

Carbon microribbon targets [10] were employed by bundling several ribbons together (each of which were 6 $\mu$m wide $\times$ 3 cm long by $3.7 \pm 0.2$ $\mu$g/cm$^2$) in order to get a sufficient counting rate. The effective target thickness, needed for carbon recoil energy loss corrections, was estimated to be $6.6 \pm 4.0$ $\mu$g/cm$^2$ from the multiple scattering width of the recoil carbon angular distributions.

The detector system consisted of two symmetric left and right arms detecting recoil carbon ions. Figure 1 shows a schematic layout of the experimental setup. Each detector arm consisted of a thin 5 $\mu$g/cm$^2$ carbon foil as a secondary electron emitter, an accelerating grid, an electrostatic mirror, and a microchannel plate (MCP) assembly, all
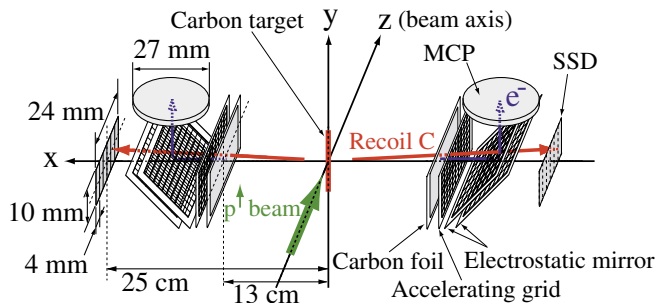
followed by a silicon strip detector (SSD). The SSD had a thickness of 400 $\mu$m, a sensitive area of 24 mm wide and 10 mm long, and was segmented into six strips of 4 mm by 10 mm. The SSD covered a polar angle of $\theta = 90.0 \pm 2.7°$ and an azimuthal angle of $\phi = \pm 1.1°$ in the laboratory frame. The MCP assembly, consisting of two layers of MCP's and a single anode, had a sensitive area of 27 mm in diameter. Recoil carbon ions passed though the carbon foil and were detected with the SSD. The SSD provided the kinetic energy and the time of flight (TOF) from the target to the SSD. Secondary electrons, emitted from the carbon foil primarily by the passage of recoil carbon ions, were accelerated and reflected to the MCP with electrostatic fields. The MCP detected those electrons and provided a better start time than the rf pulse from the AGS, but with an efficiency too low to be used in the final analysis. Data collected with the MCP's were used in systematic checks of the measurement and a background estimation.

Data were recorded for every AGS cycle. The primary trigger was a coincidence between the signal from one of the SSD strips and the rf pulse. The dead time of the data acquisition system was measured to be typically 5%. The energy calibration of each of the SSD strips was carried out with an $^{241}_{95}$Am (5.486 MeV $\alpha$ particles) radioactive source.

Low energy recoil carbon ions were clearly seen as a kinematical correlation between $E$ and $T_{SSD}$, where $E$ and $T_{SSD}$ are the energy deposit and the timing in the SSD strip, respectively. Figure 2(a) shows the correlation obtained from one of the SSD strips. Energy losses in the target, the carbon foil, and the SSD dead layer ($22.6 \pm 1.0$ $\mu$g/cm$^2$ Si equivalent) were corrected to obtain the kinetic energy of recoil carbon ions. The detector

FIG. 1 (color online). Schematic layout of the E950 experimental setup (not to scale).
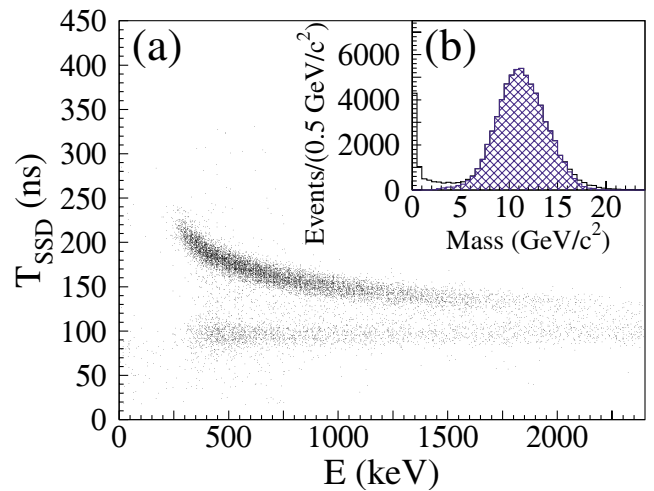
FIG. 2 (color online). (a) The correlation between the energy deposit, $E$, and the timing, $T_{SSD}$, in one of the SSD strips. Recoil carbon events are seen in the distribution at longer times. The flat band at shorter times is from background, which is also seen in the target-empty data. (b) The mass distribution in the measured $t$ range. Events selected with the 2.5-sigma mass resolution cut are shown as a hatched area.

resolution was determined from the time-energy correlation and the reconstructed mass distribution of recoil carbon events. The resolution of $T_{SSD}$ was $7.0 \pm 0.5$ ns independent of $E$ and consistent with the beam bunch width. The resolution of $(T_{SSD} - T_{MCP})$, where $T_{MCP}$ is the timing in the MCP, was 1.2–3.8 ns, decreasing with $E$. The energy resolution of the SSD, obtained from both the time resolutions and the mass distribution, was $\Delta E/E = 0.05/\sqrt{E(\text{MeV})} \oplus C$ (quadratic sum), where the constant value of $C$ varied in SSD strips from 0.05 to 0.12.

The momentum transfer in $p$C elastic scattering can be defined by the kinetic energy of the recoil carbon as $t_E$ or by the TOF from the target to the SSD as $t_T$. Taking into account detector resolution smearing, momentum transfer was defined by the resolution-weighted mean, $t = (w_E t_E + w_T t_T)/(w_E + w_T)$, where the weights, $w_E$ and $w_T$, were determined from the energy resolution and the time resolution, respectively. The calculation was dominated by $t_E$ since $w_E/(w_E + w_T)$ ranged from 0.6 to 0.9 depending upon $t$. The $t$ range covered to obtain $\mathcal{A}_N$ was $9.0 \times 10^{-3} < -t < 4.1 \times 10^{-2}$ $(\text{GeV}/c)^2$.

Recoil carbon events were identified by the mass reconstructed from the kinetic energy and the TOF from the target to the SSD. Figure 2(b) shows the mass distribution in the measured $t$ range. The mass resolution was 2.1–3.8 $\text{GeV}/c^2$ as a function of $t$. A 2.5-sigma mass resolution cut was applied to select recoil carbon events. Backgrounds in the selected recoil carbon events were estimated as a function of $t$. Backgrounds estimated from the target-empty data were 0.3%–2.7%. Backgrounds due to target fragments (dominated by $\alpha$'s) were estimated to be 0.8%–11.9% from the mass distribution reconstructed from the kinetic energy and the TOF from the carbon foil to the SSD, using $(T_{SSD} - T_{MCP})$ with the mass resolution of 1.2–2.5 $\text{GeV}/c^2$. The total background was 1.4%–13.9% and was subtracted from the selected recoil carbon events for each spin state separately. The angular distribution of the selected recoil carbon events for each $t$ was obtained from the distribution of the hit position in the SSD. The recoil angle, $\theta$, and the multiple scattering width, $\Delta\theta$, in the measured $t$ range were determined to be $89.0° < \theta < 89.7°$ and $0.8° < \Delta\theta < 1.3°$. The recoil angle as a function of $t$ was consistent with that of $p$C elastic scattering kinematics. A total of $2.2 \times 10^7$ $p$C elastic scattering events were thus identified for the $\mathcal{A}_N$ calculation.

The analyzing power of $p$C elastic scattering was determined as a function of $t$ using the formula [11],

$$\mathcal{A}_N = \frac{1}{\mathcal{P}_B} \frac{\sqrt{N_L^\uparrow \cdot N_R^\downarrow} - \sqrt{N_L^\downarrow \cdot N_R^\uparrow}}{\sqrt{N_L^\uparrow \cdot N_R^\downarrow} + \sqrt{N_L^\downarrow \cdot N_R^\uparrow}}, \quad (1)$$

where $N_L^\uparrow$ ($N_R^\downarrow$) represent the number of events in which the scattered proton was in the left (right) side and the recoil carbon was in the right (left) side to the beam axis with the polarization direction up (down). Equation (1) cancels out

TABLE I. $\mathcal{A}_N$ as a function of $t$ $(\text{GeV}/c)^2$. Errors in $t$ are the systematic error from the estimation of the energy loss at the target. The three errors in $\mathcal{A}_N$ are the statistical error, the systematic error in the raw asymmetry, and that in the beam polarization, respectively.

| $-t$ [$(\text{GeV}/c)^2$] | $\mathcal{A}_N$ |
|---|---|
| $(0.90 \pm 0.03) \times 10^{-2}$ | $(1.30 \pm 0.22 \pm 0.35 \pm 0.16) \times 10^{-2}$ |
| $(1.26 \pm 0.04) \times 10^{-2}$ | $(1.48 \pm 0.11 \pm 0.12 \pm 0.18) \times 10^{-2}$ |
| $(1.72 \pm 0.04) \times 10^{-2}$ | $(1.19 \pm 0.11 \pm 0.17 \pm 0.14) \times 10^{-2}$ |
| $(2.20 \pm 0.05) \times 10^{-2}$ | $(1.05 \pm 0.13 \pm 0.11 \pm 0.13) \times 10^{-2}$ |
| $(2.69 \pm 0.05) \times 10^{-2}$ | $(0.12 \pm 0.15 \pm 0.18 \pm 0.01) \times 10^{-2}$ |
| $(3.17 \pm 0.06) \times 10^{-2}$ | $(-0.03 \pm 0.18 \pm 0.10 \pm 0.00) \times 10^{-2}$ |
| $(3.65 \pm 0.06) \times 10^{-2}$ | $(-0.20 \pm 0.21 \pm 0.25 \pm 0.02) \times 10^{-2}$ |
| $(4.13 \pm 0.06) \times 10^{-2}$ | $(-0.15 \pm 0.24 \pm 0.29 \pm 0.02) \times 10^{-2}$ |

the acceptance difference between the left and the right detector arm and the beam intensity difference between the up and the down polarized state. Each square root represents a geometric mean of two independent measurements of the same quantity which follows the rotational symmetry of the cross section around the beam axis. The resulting $\mathcal{A}_N$ is shown in Table I and Fig. 3 and is nonzero at the lower $t$ range with high statistical precision. The systematic error in the raw asymmetry measurement was estimated from a number of possible systematic effects, mainly from the uncertainty in the event selection of recoil carbon ions. The time-dependent variation of the measured raw asymmetry was consistent with a statistical fluctuation, $\chi^2/\text{d.o.f.} = 1.16$. The normalization error in the $\mathcal{P}_B$ measurement was 12%, which comes from the uncertainty of $\mathcal{A}_N^{pp}$. Our result of $\mathcal{A}_N$ is in marked disagreement with
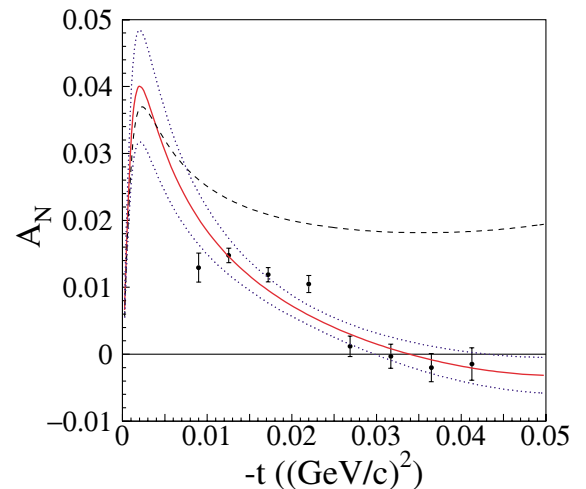


FIG. 3 (color online). The analyzing power, $\mathcal{A}_N$, for $p$C elastic scattering in the CNI region. The error bars on the data points are statistical only. The solid line is the fitted function from theory [4]. The dotted lines are the 1-sigma error band of the fitting result. The dashed line is the theoretical function with no hadronic spin-flip amplitude ($r_5 = 0$).
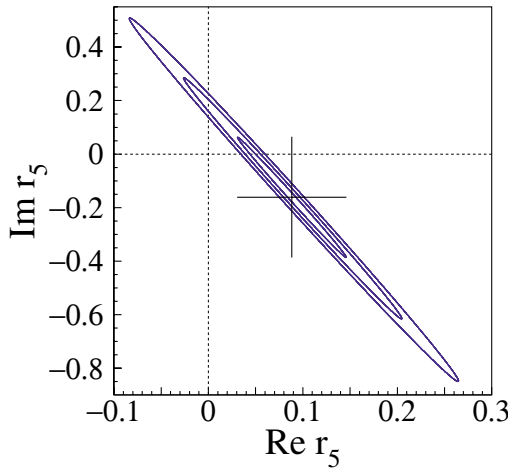
FIG. 4 (color online).  Ratio of hadronic spin-flip to nonflip amplitude, $r_5$, and the 1-, 2-, and 3-sigma contours of $\chi^2$.

the model-independent calculation with no hadronic spin-flip amplitude ($r_5 = 0$) shown in Fig. 3 [4,12].

The ratio of hadronic spin-flip to nonflip amplitude, $r_5$, was determined by fitting the measured $\mathcal{A}_N$ with the theoretical formula of Ref. [4]. Errors used for $\mathcal{A}_N$ in the fitting were the linear sum of three errors in Table I. The fitted function with 1-sigma error band is shown in Fig. 3. The best fit gave a value of $r_5$ as $\mathrm{Re}r_5 = 0.088 \pm 0.058$ and $\mathrm{Im}r_5 = -0.161 \pm 0.226$ with $\chi^2/\mathrm{d.o.f.} = 0.57$. The result of $r_5$ and its associated $\chi^2$ contours are shown in Fig. 4.

The magnitude of the hadronic spin-flip amplitude has been a long-standing question. The E581/E704 experiment at Fermilab measured $\mathcal{A}_N$ for $pp$ elastic scattering in the CNI region at 200 GeV/$c$ [13]. The result was consistent with no hadronic spin-flip amplitude within the limited statistical precision. Theoretical estimates of $r_5$ based on several approaches have been made [2], indicating $|r_5| < 0.15$ from the E581/E704 result and $|r_5| < 0.10$ for the RHIC energy range of $\sqrt{s} = 50$–500 GeV. The present results using the carbon target provide a better determination of spin properties of scattering amplitudes which may help to reveal the dynamical mechanisms for scattering in the high energy asymptotic region. To understand the asymptotic spin properties of scattering amplitudes more systematically, it is necessary to measure $\mathcal{A}_N$ in the CNI region at higher energies where the Pomeron amplitude is dominant. This may be performed by our method at RHIC.

In conclusion, we measured for the first time the $\mathcal{A}_N$ for $p$C elastic scattering in the CNI region of $9.0 \times 10^{-3} < -t < 4.1 \times 10^{-2}$ (GeV/$c$)$^2$ at 21.7 GeV/$c$ with high statistical precision. A nonzero value of $r_5$ was obtained from $\mathcal{A}_N$ to be $\mathrm{Re}r_5 = 0.088 \pm 0.058$ and $\mathrm{Im}r_5 = -0.161 \pm$

0.226. The experimental method used is applicable to high energy proton polarimetry at RHIC [14].

*Present address: RIKEN (The Institute of Physical and Chemical Research), Wako, Saitama 351-0198, Japan.
†Present address: Department of Physics, Rikkyo University, Toshima, Tokyo 171-8501, Japan.
‡Present address: Department of Physics, Kyoto University, Kyoto 606-8502, Japan.
§Present address: Fermi National Accelerator Laboratory, Batavia, IL 60510.
‖Present address: Department of Physics, Osaka City University, Osaka 55-8585, Japan.
¶Present address: Department of Nuclear Physics, China Institute of Atomic Energy, Beijing 102413, China.

[1] B. Z. Kopeliovich and L. I. Lapidus, Sov. J. Nucl. Phys. **19**, 114 (1974); N. H. Buttimore, E. Gotsman, and E. Leader, Phys. Rev. D **18**, 694 (1978).
[2] N. H. Buttimore *et al.* Phys. Rev. D **59**, 114010 (1999), and references therein.
[3] N. H. Buttimore, in *High Energy Spin Physics*, edited by G. M. Bunce, AIP Conf. Proc. No. 95 (AIP, New York, 1983), p. 634.
[4] B. Z. Kopeliovich and T. L. Trueman, Phys. Rev. D **64**, 034004 (2001).
[5] B. Z. Kopeliovich and B. G. Zakharov, Phys. Lett. B **226**, 156 (1989); T. L. Trueman, hep-ph/9610429.
[6] Physics of Polarimetry at RHIC, Proceedings of RIKEN BNL Research Center Workshop 1998, Report No. BNL-65926.
[7] H. Huang *et al.*, Phys. Rev. Lett. **73**, 2982 (1994).
[8] M. Bai *et al.*, Phys. Rev. Lett. **80**, 4673 (1998).
[9] K. Krueger *et al.*, Phys. Lett. B **459**, 412 (1999); C. E. Allgower *et al.*, Phys. Rev. D **65**, 092008 (2002).
[10] W. R. Lozowski and J. D. Hudson, Nucl. Instrum. Methods Phys Res., Sect. A **303**, 34 (1991).
[11] G. G. Ohlsen and P. W. Keaton, Jr., Nucl. Instrum. Methods **109**, 41 (1973).
[12] B. Z. Kopeliovich and T. L. Trueman (private communication). The main theoretical uncertainty is in the realistic parametrization for the nuclear density distribution used in Ref. [4]. Both the harmonic oscillator and the Woods-Saxon parametrization gave the identical result.
[13] N. Akchurin *et al.*, Phys. Lett. B **229**, 299 (1989); N. Akchurin *et al.*, Phys. Rev. D **48**, 3026 (1993).
[14] Based on this measurement, the "$p$C CNI polarimeter" was constructed and installed in the RHIC ring.